

01 Jan 2003

Control of Cascaded Multi-level Inverters

Keith Corzine
Missouri University of Science and Technology

Fang Zheng Peng

J. Wang

M. W. Wielebski

Follow this and additional works at: https://scholarsmine.mst.edu/ele_comeng_facwork



Part of the [Electrical and Computer Engineering Commons](#)

Recommended Citation

K. Corzine et al., "Control of Cascaded Multi-level Inverters," *Proceedings of the IEEE International Electric Machines and Drives Conference, 2003*, Institute of Electrical and Electronics Engineers (IEEE), Jan 2003. The definitive version is available at <https://doi.org/10.1109/IEMDC.2003.1210657>

This Article - Conference proceedings is brought to you for free and open access by Scholars' Mine. It has been accepted for inclusion in Electrical and Computer Engineering Faculty Research & Creative Works by an authorized administrator of Scholars' Mine. This work is protected by U. S. Copyright Law. Unauthorized use including reproduction for redistribution requires the permission of the copyright holder. For more information, please contact scholarsmine@mst.edu.

Control of Cascaded Multi-Level Inverters

K.A. Corzine
Member, IEEE

M.W. Wielebski
Student Member, IEEE

F.Z. Peng
Senior Member, IEEE

J. Wang
Student Member, IEEE

Department of Electrical Engineering
University of Wisconsin - Milwaukee
3200 N. Cramer Street
Milwaukee, WI 53211, USA

Department of Electrical Engineering
Michigan State University
2120 Engineering Building
East Lansing, MI 48824, USA

Abstract - A new type of multi-level inverter is introduced which is created by cascading two three-phase three-level inverters using the load connection. This new inverter can operate as a nine-level inverter and naturally splits the power conversion into a higher-voltage lower-frequency inverter and a lower-voltage higher-frequency inverter. This type of system presents particular advantages to Naval ship propulsion systems which rely on high power quality, survivable drives. New control methods are described involving both joint and separate control of the individual three-level inverters. Simulation results demonstrate the effectiveness of both controls. A laboratory set-up at the Naval Surface Warfare Center power electronics laboratory was used to validate the proposed joint-inverter control. Due to the effect of compounding levels in the cascaded inverter, a high number of levels are available resulting in a voltage THD of 9% (without filtering).

Keywords: Multi-level, hybrid, neutral-point clamped, medium-voltage, cascaded H-bridge.

I. INTRODUCTION

The concept of multi-level inverters, introduced about 20 years ago [1, 2], entails performing power conversion in multiple voltage steps to obtain improved power quality, lower switching losses, better electromagnetic compatibility, and higher voltage capability. Considering these advantages, multi-level converters have been gaining considerable popularity in recent years [3-18]. The benefits are especially clear for medium-voltage drives in industrial applications [7, 9] and are being considered for future Naval ship propulsion systems. In fact, several IEEE conferences now hold entire sessions on multi-level power conversion.

Several topologies for multi-level inverters have been proposed over the years; the most popular being the diode-clamped [3,4], flying capacitor [5, 6] and cascaded H-bridge [7-10] structures. One aspect which sets the cascaded H-bridge apart from other multi-level inverters is the capability of utilizing different dc voltages on the individual H-bridge cells which results in splitting the power conversion amongst higher-voltage lower-frequency and lower-voltage higher-frequency inverters [9,10]. An alternate method of cascading inverters involves series connection of two three-phase inverters through the neutral point of the load. Past research has shown this concept for cascading two-level inverters [11-15] and multi-level inverters [16-18]. An advantage of this approach is that isolated sources are not required for each phase. It should be noted that cascaded inverter systems can be considered from a number of

different viewpoints. Considering the cascaded inverter to be one unit, it can be seen that a higher number of voltage levels are available for a given number of semiconductor devices. Considering the system as separate inverters, the cascaded design can be regarded as a combination of a bulk power (higher-voltage) inverter and a conditioning (lower-power) inverter. An alternate viewpoint is to consider the conditioning inverter as an active filter and the bulk inverter as the drive inverter. In any case, the cascaded multi-level inverter has several advantages for Naval ship propulsion systems. One advantage is that cascaded inverters provide a compounding of voltage levels leading to extremely low harmonics necessary to meet low acoustic noise requirements. Another advantage is that the bulk inverter may be commercial-off-the-shelf; requiring that only the lower-power condition inverter to be custom made. Yet another advantage is that the cascaded design avoids a large number of isolated voltage sources which would be cumbersome in shipboard power systems. An additional advantage is that the dual inverter structure may be useful for redundancy providing remedial operation for survivability. Furthermore, in Naval applications, the propulsion motor is typically custom built and can be readily made to have access to both ends of each winding.

This paper reports the development of new control methods for cascaded multi-level inverters. In particular, capacitor voltage regulation methods are introduced resulting in a cascaded inverter which only requires one dc source. The new control methods are applied to a topology where two three-level inverters are cascaded. Simulation and laboratory measurements are presented which demonstrate the effectiveness of the proposed control.

II. CASCADED MULTI-LEVEL INVERTERS

The cascade-3/3 inverter is shown in Figure 1. This topology is constructed by connecting a three-level inverter to both sides of the motor windings. As a practical matter, the inverters may have any number of voltage levels as described in the literature [17]. Assuming that the capacitors are charged to half of their respective dc bus voltage, the line-to-ground voltages of the upper and lower voltage may be expressed as

$$\begin{bmatrix} v_{ag} & v_{bg} & v_{cg} \end{bmatrix}^T = \begin{bmatrix} s_a & s_b & s_c \end{bmatrix}^T \frac{V_{dc}}{2} \quad (1)$$

$$\begin{bmatrix} v_{agx} & v_{bgx} & v_{cgx} \end{bmatrix}^T = \begin{bmatrix} s_{ax} & s_{bx} & s_{cx} \end{bmatrix}^T \frac{V_{dcx}}{2} \quad (2)$$

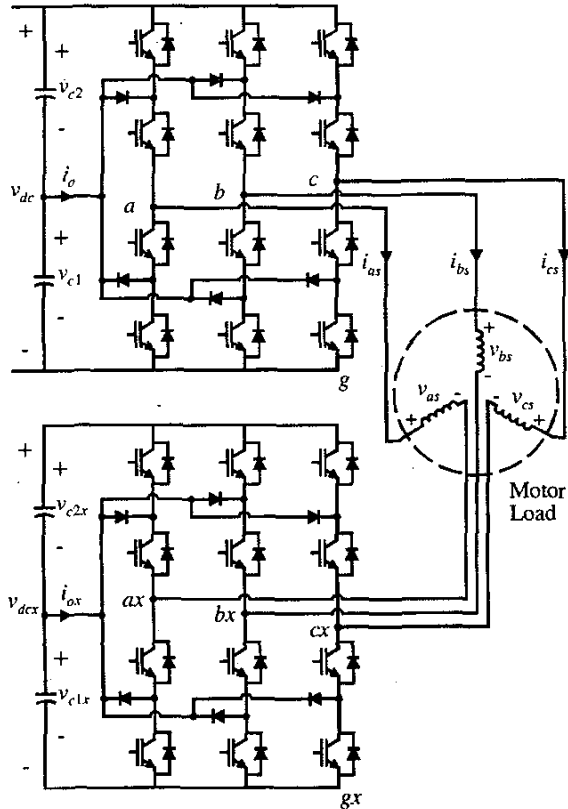


Figure 1. The cascade-3/3 multi-level inverter.

where s_a , s_b , and s_c are the switching states for the upper inverter and s_{ax} , s_{bx} , and s_{cx} are the switching states for the lower inverter. For three-level inverters, the switching states correspond to the line-to-ground voltage levels and can have the values 0, 1 or 2. The phase voltages of the load may be expressed in terms of the line-to-ground voltages as [19]

$$\begin{bmatrix} v_{as} \\ v_{bs} \\ v_{cs} \end{bmatrix} = \frac{1}{3} \begin{bmatrix} 2 & -1 & -1 \\ -1 & 2 & -1 \\ -1 & -1 & 2 \end{bmatrix} \begin{bmatrix} v_{ag} - v_{agx} \\ v_{bg} - v_{bgx} \\ v_{cg} - v_{cgx} \end{bmatrix} \quad (3)$$

The effective line-to-line load voltages may be expressed in terms of the phase voltages as

$$\begin{bmatrix} v_{abs} \\ v_{bcs} \\ v_{cas} \end{bmatrix} = \begin{bmatrix} 1 & -1 & 0 \\ 0 & 1 & -1 \\ -1 & 0 & 1 \end{bmatrix} \begin{bmatrix} v_{as} \\ v_{bs} \\ v_{cs} \end{bmatrix} \quad (4)$$

It is often insightful to look at the voltage vector plot of a multi-level inverter which can be accomplished by plotting the phase voltages in the d - q stationary reference frame for all possible

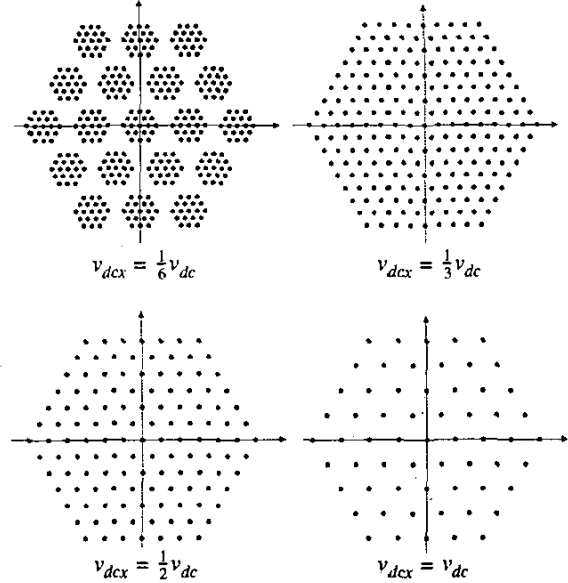


Figure 2. Cascade-3/3 inverter vector plots.

combinations of switching states [11]. In the case of the cascaded multi-level inverter, vector plots vary widely depending on the ratio of the dc voltages. Figure 2 shows the voltage vector plots for the cascade-3/3 inverter for several dc voltage ratios. Therein, the axes of each subplot are the same as those shown in Figure 3. When the voltage ratio is set to

$v_{dcx} = \frac{v_{dc}}{6}$, the vector plot appears as that of several three-level vector plots arranged in a three-level pattern. This is to be expected when cascading two three-level inverters as the amplitude of the small vector patterns depends on the dc voltage v_{dcx} . Incidentally, if v_{dcx} is set to zero, the amplitude of its vectors goes to zero and the overall vector plot is that of a three-level inverter (the lower inverter turns into a neutral connection).

The next ratio is $v_{dcx} = \frac{v_{dc}}{3}$ where there is some overlap of the voltage vectors and the vector plot is the same as that of a nine-level inverter. As it turns out, nine levels is the largest number of voltage levels that the cascade-3/3 inverter is capable of emulating. For this reason, this mode of operation is referred to as maximal distention [11,17]. In general, the voltage ratio which yields maximal distention for an arbitrary number of voltage levels is [17]

$$\frac{v_{dcx}}{v_{dc}} = \frac{n_x - 1}{n n_x - n_x} \quad (5)$$

where n and n_x are the voltage levels of the upper and lower inverter respectively. As shown in Figure 2, if the voltage ratio is increased further to $v_{dcx} = \frac{v_{dc}}{2}$ and $v_{dcx} = v_{dc}$, the cascade-3/3 inverter can operate as a seven-level and five-level inverter respectively. However, these modes of operation are not as

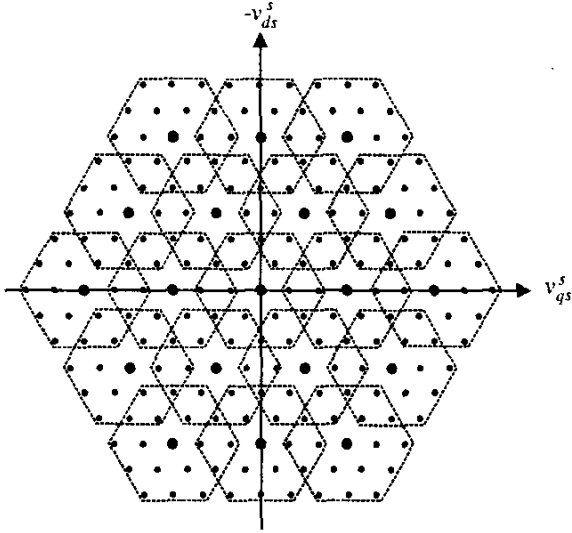


Figure 3. Cascade-3/3 vector plot for maximal distortion.

desirable as that of maximal distortion which yields the highest power quality through lower voltage steps.

III. CASCADE-3/3 INVERTER CONTROL

Before considering specific modulation and capacitor voltage regulation strategies, it is instructive to examine the cascade-3/3 inverter vector plot shown in Figure 3 in detail. Therein, the vectors produced by the upper inverter are denoted as being slightly larger than the other vectors. The small three-level vector plots produced by the lower inverter are indicated by the dashed hexagons. One of the significant features of the controls developed herein is the ability to regulate the dc voltage v_{dcx} so that only one dc source is required. This can be accomplished through redundant selection of inverter switching states. Figure 3 shows overlap amongst the smaller hexagons and where this overlap occurs there is a choice as to the realization of the voltage vectors. This choice can be made with regard to the power flow in the lower inverter [14] so that the dc voltage v_{dcx} remains at one-third of v_{dc} . As can be seen from Figure 3, a considerable amount of overlap occurs for vectors toward the inside of the vector plot and the full dc voltage v_{dc} may be utilized while regulating the lower inverter capacitor voltage. Towards the outside of the vector plot, the overlap is not present for many vectors and in this case, the power flow can not be used to maintain v_{dcx} . This results in a limitation of operating region within the upper inverter vectors (larger vectors in Figure 3). Considering the number of lower inverter vectors in-between the upper inverter vectors, it can be seen that this limitation will result in seven-level operation. However, only one dc source is required and that dc voltage can be fully utilized.

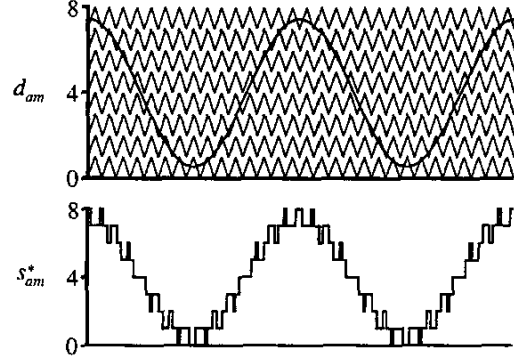


Figure 4. Nine-level triangle modulation.

A. Joint-Inverter Control

The method of joint inverter control proposed herein utilized nine-level modulation followed by a redundant state selection (RSS) table for capacitor voltage balancing. The process of nine-level modulation is shown for the a-phase in Figure 4 where a modified duty cycle d_{am} is compared to eight triangle waveforms to produce the a-phase commanded switching state s_{am}^* . The comparison rules assert that the switching state be equal to the number of triangle waveforms that the modified duty cycle is greater than. The modified duty cycle is calculated as

$$d_{am} = 4 \left[1 + \frac{3\hat{m}}{4} \cos(\theta_e) \right] \quad (6)$$

where the duty cycle has been modified from the traditional definition so that it ranges from 0 to 8 (the number of levels minus 1) and the modulation index \hat{m} represents the percent of voltage utilization of v_{dc} and ranges from 0 to 1. The angle is the electrical angle which corresponds to the commanded frequency. The duty cycles of the b- and c-phase are similar to that of (6) with 120° and 240° offset in the electrical angle respectively. Typically, all three duty cycles are compared to the same set of triangle waveforms. To produce commanded switching states s_{am}^* , s_{bm}^* , and s_{cm}^* .

The modulation is typically programmed in a digital signal processor (DSP) and may be followed by an RSS table located in either the DSP or in a programmable logic device (PLD). Figure 5 shows the RSS table structure for this system. The inputs (address) of the table are the commanded switching states from the modulator as well as digital flags which represent the state of the system. The flags I_a , I_b , and I_c indicate the current direction and are 1 for positive and 0 for negative values of i_{as} , i_{bs} , and i_{cs} respectively. The capacitor voltage flags represent voltage balance and are defined by

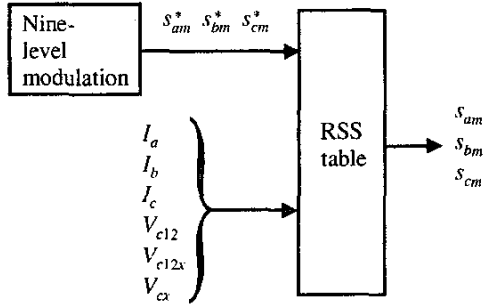


Figure 5. Redundant state selection implementation.

$$V_{c12} = \begin{cases} 1 & v_{c1} \geq v_{c2} \\ 0 & v_{c1} < v_{c2} \end{cases} \quad (7)$$

$$V_{c12x} = \begin{cases} 1 & v_{c1x} \geq v_{c2x} \\ 0 & v_{c1x} < v_{c2x} \end{cases} \quad (8)$$

$$V_{cx} = \begin{cases} 1 & v_{dcx} \geq \frac{1}{3}v_{dc} \\ 0 & v_{dcx} < \frac{1}{3}v_{dc} \end{cases} \quad (9)$$

The RSS table output is the switching state for each phase. This can be related to the switching states of the individual inverters by consideration of the line-to-ground voltages [16]. Table I shows this relationship for the a -phase.

s_{am}	0	1	2	3	4	5	6	7	8
s_a	0	0	0	1	1	1	2	2	2
s_{ax}	2	1	0	2	1	0	2	1	0

Identical relationships apply for determining the b - and c -phase inverter switching states.

The final consideration for this control is the method of generating the RSS table. For this, a program was written to evaluate the redundant states for all possible combinations of the RSS table inputs. Each combination of inputs was evaluated in the following way. First the number of redundant switching states was identified by

$$n_{RSS} = n \cdot n_x - (s_{max} - s_{min}) \quad (10)$$

where s_{max} and s_{min} are the maximum switching states from the modulator or

$$s_{max} = \text{MAX}(s_{am}^*, s_{bm}^*, s_{cm}^*) \quad (11)$$

$$s_{min} = \text{MIN}(s_{am}^*, s_{bm}^*, s_{cm}^*) \quad (12)$$

To obtain the first redundant state, s_{min} is subtracted from the switching states of all three phases. The other states are obtained by adding 1 to all three phases (changing the common-mode or zero sequence term) until all redundant states are evaluated. For each redundant state, the contribution to power from the lower inverter is found by first deterring the switching states corresponding to that inverter from Table I. Next, the contribution to the line-to-ground voltages can be evaluated using

$$\begin{bmatrix} v_{asx} \\ v_{bsx} \\ v_{csx} \end{bmatrix} = \frac{1}{3} \begin{bmatrix} 2 & -1 & -1 \\ -1 & 2 & -1 \\ -1 & -1 & 2 \end{bmatrix} \begin{bmatrix} v_{agx} \\ v_{bgx} \\ v_{cgx} \end{bmatrix} \quad (13)$$

Finally, the contribution of the lower inverter power may be expressed as

$$p_x = v_{asx}(1 - 2I_a) + v_{bsx}(1 - 2I_b) + v_{csx}(1 - 2I_c) \quad (14)$$

It should be noted that (14) can not calculate the exact power since the current flags only represent the current direction. However, for high power factors (14) can be used to determine the direction of power flow. If the direction is positive (out of the inverter) and the capacitor is overcharged (or $V_{cx} = 1$) the redundant state will help regulate the capacitor voltage. Similarly, if the power direction is negative and the capacitor is undercharged, the redundant state will help regulate the capacitor voltage. Any redundant states which help the balance situation are given a priority of 4. The reason for this is that some priority will be added to the redundant states which also help the capacitor voltage balancing within the inverters. Evaluating this voltage balance amounts to determining the direction of the current in each inverter which flows out of the capacitor junction (currents i_o and i_{ox} in Figure 1). For each redundant state, the junction current is determined by using Table I to determine which phases are connected to the junction and then adding the current depending on the current direction flags. The direction of the junction currents can be used with the capacitor balance information (V_{c12} and V_{c12x}) to determine if the redundant state helps the voltage balance. For the upper inverter, cases which help the balance have their priority increased by 1. For the lower inverter, cases which help the balance have their priority increased by 2. This choice is arbitrary, but was made based on simulation results. After evaluating all of the redundant states, the one with the highest priority is selected for the RSS table data.

The cascade-3/3 inverter was simulated using the proposed control. In the simulation, the dc voltage was set to $v_{dc} = 601.8V$. The controller modulation index was $\hat{m} = 1$ with a commanded frequency of 60Hz. The load was a resistive-inductive load with $R = 11\Omega$ and $L = 17.5mH$. Figure 6 shows the simulation results. Therein, the a -phase upper and lower line-to-ground voltages v_{ag} and v_{agx} are shown followed

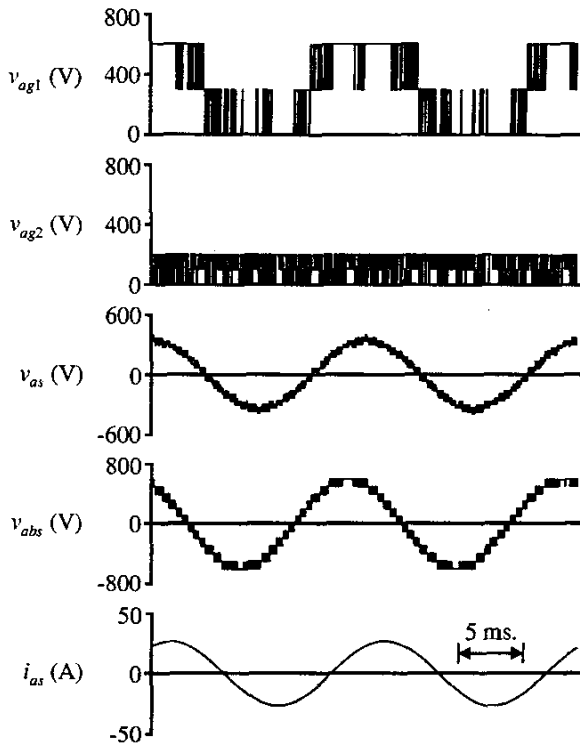


Figure 6. Cascade-3/3 inverter simulation results.

by the load voltage v_{as} , the line-to-line voltage v_{abs} as defined by (4), and the phase current i_{as} . From the line-to-ground voltages, it can be seen that there is a natural split between higher-voltage lower-frequency and lower-voltage higher-frequency. The line-to-ground voltages also demonstrate the effectiveness of the capacitor voltage balancing control. From the line-to-line voltage, the effective seven-level operation can be seen (6 positive levels, 6 negative levels, and 0). For this simulation, the output power was 23kW and the THD of the phase and line-to-line voltages were $\text{THD}(v_{as}) = 9.42\%$ and $\text{THD}(v_{abs}) = 9.34\%$.

B. Separate Inverter Control

Unlike the joint-inverter control, the proposed separate inverter control utilizes isolated algorithms for the bulk and conditioning inverter. The bulk inverter is controlled by the staircase or low-frequency PWM method to provide power needed to drive the motor, whereas the conditioning inverter utilizes high-frequency PWM to shape motor voltage and current and achieve high performance drive with low current and torque ripple. One advantage of the separate inverter control is that no communication is needed between the two inverters, thus making it possible to use commercial-off-the-shelf motor drive inverters. It should be noted that, as with the joint-inverter

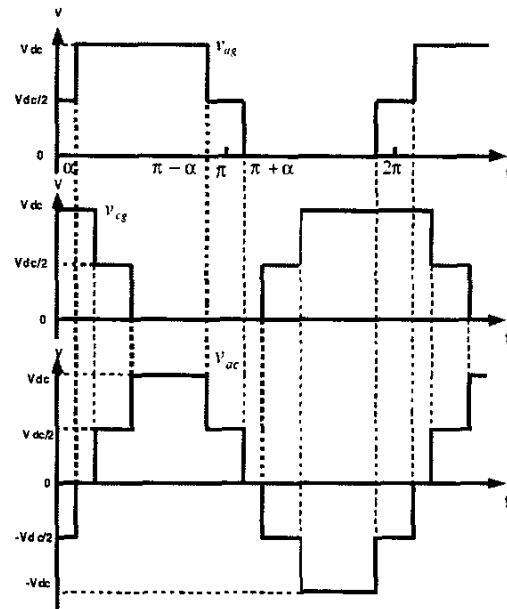


Figure 7. Staircase control of the bulk inverter.

control the conditioning inverter does not need a power supply, thus acting like an active filter.

The process of the staircase control of the bulk inverter is shown in Figure 7, where the angle α is controlled to produce the staircase voltage waveform. Therein, the phase voltages v_{ag} and v_{cg} and the line-to-line voltage v_{ac} are shown. The amplitude of any odd n^{th} harmonic of the phase voltage can be expressed as

$$v_n = \frac{2v_{dc}}{n\pi} \cos(\alpha) \quad (15)$$

where n is an odd harmonic order, the amplitudes of all even harmonics being zero. The amplitude of the fundamental component in the phase voltage can be calculated as

$$v_f = \frac{2v_{dc}}{\pi} \cos(\alpha). \quad (16)$$

According to Figure 7, α must satisfy $0 < \alpha < \frac{\pi}{2}$.

The conditioning inverter functions like a series active power filter to compensate the harmonic voltage produced by the bulk inverter. In the time-domain, this harmonic can be computed for the a -phase as

$$v_{ag,h} = v_{ag} - v_{ag,f} \quad (17)$$

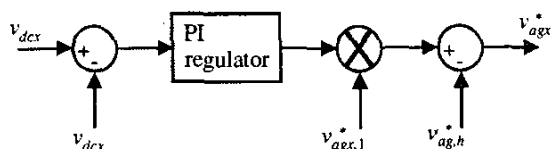


Figure 8. Conditioning inverter control diagram.

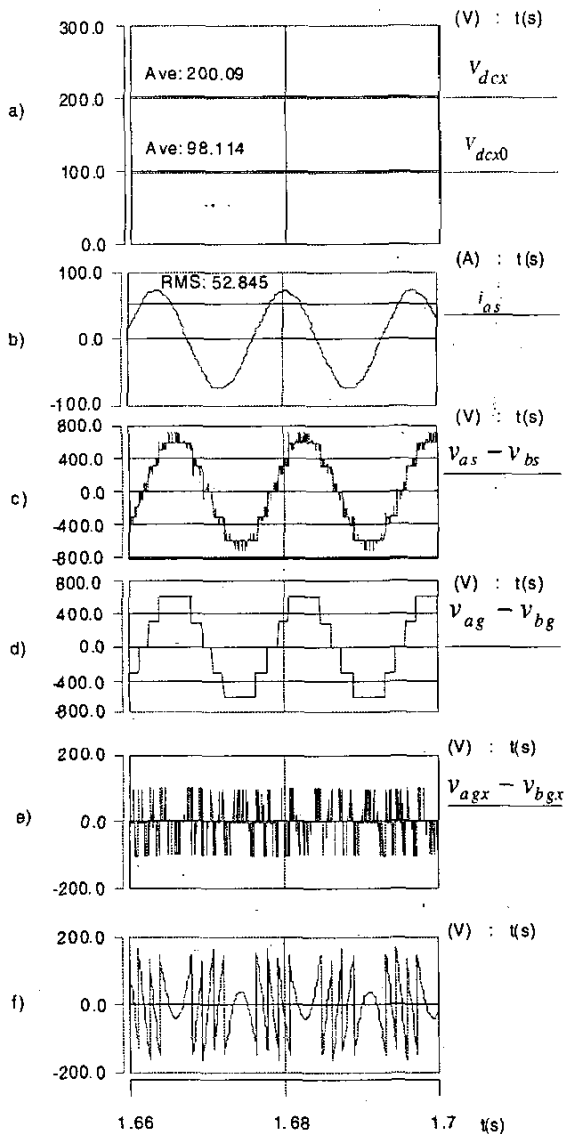


Figure 9. Separate control simulation results.

where $v_{ag,f}$ is the fundamental component of v_{ag} . The harmonics for the b - and c -phase can be computed in the same way.

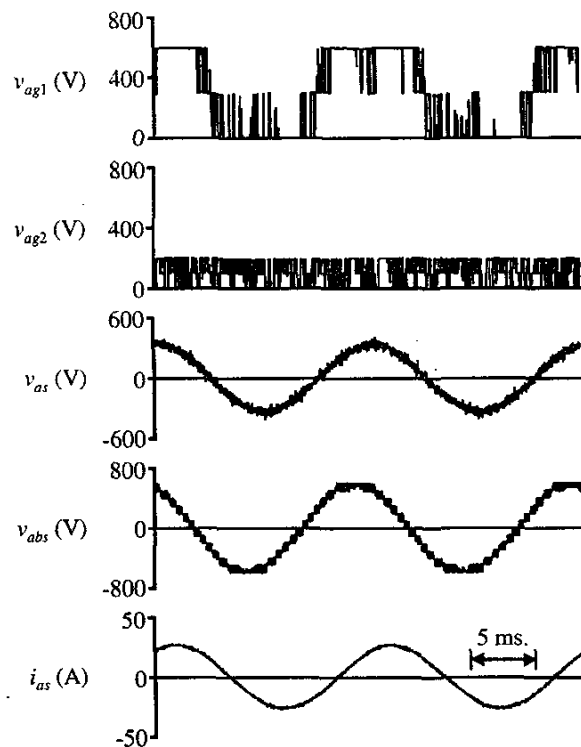


Figure 10. Cascade-3/3 inverter measurements.

Another consideration of the separate inverter control is the dc voltage control of the conditioning inverter. In order to maintain maximal distortion, the dc capacitor voltage on the conditioning inverter should be kept at one third of the dc voltage of the bulk inverter. To achieve this, a straightforward PI control is adopted to regulate active power flow into the conditioning inverter. The control scheme of the conditioning inverter is shown in Figure 8 for the a -phase. Therein, v_{dc}^* is the DC voltage reference, which is set to one third of v_{dc} . The voltage $v_{ag,1}^*$ is a unit sinusoidal wave, which has the same phase angle with the phase voltage $v_{ag,f}$. The resulting reference voltage is used as an input for a PWM modulator for the conditioning inverter. Similar control channels are used for the b - and c -phase.

Figure 9 shows simulation results of the cascade multi-level converter using the separate control, in which a) is the dc voltage of the conditioning inverter; b) is the motor current; c) is the total motor line-line voltage; d) is the bulk inverter line-line voltage; e) is the conditioning inverter line-line voltage and f) is the harmonics in the line-line voltage of the bulk inverter. In simulation, v_{dc} was set to 600 V and α was set to 15° . It can be seen that the dc link voltage of the conditioning inverter is kept at one third of the dc voltage of the bulk inverter. The total line-to-line voltage is improved from the bulk inverter five-level

waveform by the conditioning inverter and the maximal distortion of the cascaded inverter is realized.

IV. LABORATORY VALIDATION

The cascade-3/3 inverter was constructed in the power electronics laboratory at the Naval Surface Warfare Center (NSWC) in Philadelphia. Joint inverter control was used and the operating conditions were the same as those described in the simulation in Section III A. Figure 10 shows the laboratory measurements displaying the same system variables as Figure 6. As can be seen, the measurements are nearly the same as the simulation with the exception of the ripple in the phase current which is higher in lab measurements due to high-frequency effects (inter-winding capacitance and etc.) which were not included in the simulation. From the measured data, the THDs were $\text{THD}(v_{as}) = 9.00\%$ and $\text{THD}(v_{abs}) = 8.14\%$.

V. CONCLUSION

This paper has studied a new type of multi-level inverter which consists of two three-phase three-level inverters cascaded through the load connections. Two types of control were developed for this inverter. One relies on controlling the two three-level inverters jointly and the other uses separate controls. Both controls included capacitor voltage balancing so that a dc source was needed for only one three-level inverter. Simulation results demonstrate the effectiveness of each control. The joint control was validated with laboratory measurements on a 23kW inverter system.

ACKNOWLEDGEMENT

The authors wish to express their gratitude for support of this research effort by Tom Fikse at the Naval Surface Warfare Center in Philadelphia and Tom Calvert at the Office of Naval Research.

REFERENCES

- R.H. Baker, *High-Voltage Converter Circuit*, U.S. Patent Number 4,203,151, May 1980.
 - A. Nabe, I. Takahashi, and H. Akagi, "A New Neutral-Point Clamped PWM Inverter," *Proceedings of the IEEE Industry Applications Society Conference*, pages 761-766, September / October 1980.
 - M. Fracchia, T. Ghiara, M. Marchesoni, and M. Mazzucchelli, "Optimized Modulation Techniques for the Generalized N-Level Converter," *Proceedings of the IEEE Power Electronics Specialist Conference*, pages 1205-1213, Madrid Spain, 1992.
 - K.A. Corzine and J.R. Baker, "Reduced Parts-Count Multi-Level Rectifiers," *IEEE Transactions on Industrial Electronics*, volume 49, issue 4, pages 766-774, August 2002.
 - F. Richardeau, P. Baudesson and T. Meynard, "Failures-Tolerance and Remedial Strategies of a PWM Multicell Inverter", *Proceedings of the IEEE Power Electronics Specialist Conference*, volume 2, pages 649-654, Galway Ireland, June 2000.
 - F.Z. Peng, "A Generalized Multilevel Inverter Topology with Self Voltage Balancing," *IEEE Transactions on Industry Applications*, volume 37, number 2, pages 611-618, March/April 2001.
 - P.W. Hammond, *Medium Voltage PWM Drive and Method*, U.S. Patent Number: 5,625,545, April 1997.
 - F.Z. Peng, J.W. McKeever, and D.J. Adams, "A Power Line Conditioner Using Cascade Multilevel Inverters for Distribution Systems," *Proceedings of the IEEE Industry Applications Society Conference*, volume 2, pages 1316-1321, 1997.
 - M.D. Manjrekar, P.K. Steimer, and T.A. Lipo, "Hybrid Multilevel Power Conversion System: A Competitive Solution for High-Power Applications," *IEEE Transactions on Industry Applications*, volume 36, number 3, pages 834-841, May/June 2000.
 - K.A. Corzine and Y.L. Familiant, "A New Cascaded Multi-Level H-Bridge Drive," *IEEE Transactions on Power Electronics*, volume 17, number 1, pages 125-131, January 2002.
 - K.A. Corzine, S.D. Sudhoff, and C.A. Whitcomb, "Performance Characteristics of a Cascaded Two-Level Converter", *IEEE Transactions on Energy Conversion*, volume 14, number 3, pages 433-439, September 1999.
 - T. Salzmann, J. Wokusch, T. Greif, and H.J. Muller, *Air-Cooled Power Converter, Drive Device for Rolling Stands, and Power Converter System*, U.S. Patent Number 6,262,906.
 - G. Shivakumar, K. Gopakumar, S.K. Sinha, A. Pittet, and V.T. Ranganathan, "Space Vector PWM Control of Dual Inverter Fed Open-End Winding Induction Motor Drive," *European Power Electronics Journal*, volume 12, number 1, pages 9-18, December 2001.
 - E.G. Shivakumar, K. Gopakumar, S.K. Sinha, A. Pittet, and V.T. Ranganathan, "Space Vector PWM Control of Dual Inverter Fed Open-End Winding Induction Motor Drive," *European Power Electronics Journal*, volume 12, number 1, pages 9-18, February 2002.
 - K.K. Mohaparta, V.T. Somasekhar, and K. Gopakumar, "A Harmonic Elimination Scheme for an Open-End Winding Induction Motor Drive Fed from Two Inverters Using Asymmetrical D.C. Link Voltages," *European Power Electronics Journal*, volume 12, number 4, pages 28-35, September / October / November 2002.
 - K.A. Corzine, *Topology and Control of Cascaded Multi-Level Converters*, Ph.D. Dissertation, University of Missouri - Rolla, 1997.
 - K.A. Corzine and S.D. Sudhoff, "High State Count Power Converters: an Alternate Direction in Power Electronics Technology," *SAE Transactions, Journal of Aerospace*, Section 1, pages 124-135, 1998.
 - Y. Kawabata, M. Nasu, T. Nomoto, E.C. Ejiogu, T. Kawabata, "High-Efficiency and Low Acoustic Noise Drive System Using Open-Winding AC Motor and Two Space-Vector-Modulated Inverters," *IEEE Transactions on Industrial Electronics*, volume 49, issue 4, pages 783-789, August 2002.
 - P.C. Krause, O. Wasynczuk, and S.D. Sudhoff, *Analysis of Electric Machinery and Drive Systems*, IEEE Press, 2002.
- Keith A. Corzine received the BSEE, MSEE, and Ph.D. degrees from the University of Missouri - Rolla in 1992 and 1994, and 1997 respectively. In the Fall of 1997 he joined the University of Wisconsin - Milwaukee where he is now an Associate Professor. His research interests include power electronics, motor drives, Naval ship propulsion systems, and electric machinery analysis. Contact: Keith@Corzine.net
- Mike W. Wielebski received the BSEE degree from the University of Wisconsin - Milwaukee in 2002 and is now pursuing the MSEE degree. His research specialty is in the area of digital mot or control and multi-level converters. Contact: wemilk@uwm.edu
- Fang Z. Peng received the B.S. degree from Wuhan University, Wuhan, China in 1983 and the M.S. and Ph.D. degrees from Nagaoka University of Technology, Nagaoka Japan, in 1987 and 1990, respectively, all in electrical engineering. From 1990 to 1992, he was a Research Scientist with Toyo Electric Manufacturing Company, Ltd., where he was engaged in research and development of active power filters, flexible ac transmission systems (FACTS) applications, and motor drives. From 1992 to 1994, he was a Research Assistant Professor at Tokyo Institute of Technology, where initiated a multilevel inverter program for FACTS applications and speed-sensorless vector control project. From 1994 to 1997, he was a Research Assistant Professor at the University of Tennessee, Knoxville, working for Oak Ridge National Laboratory (ORNL). From 1997 to 2000 he was a Senior Staff Member at ORNL and Lead (principal) Scientist of the Power Electronics and Electric Machinery Research Center. In 2000, he joined Michigan State University, East Lansing, as an Associate Professor in the Department of Electrical and Computer Engineering. He is the holder of ten patents. Contact: fzpeng@egr.msu.edu
- Jin Wang received the M.S. and B.S. degrees in electrical engineering from Wuhan University and Xi'an Jiaotong University respectively. He is presently a Ph.D. student at Michigan State University where he has been working on multi-level converters, active power filters, and DSP inverter control. Contact: Wangjin4@egr.msu.edu